Published online 6 January 2021

NAR Cancer, 2021, Vol. 3, No. 1 **1**
doi: 10.1093/narcan/zcaa040

A genome-wide strategy to identify causes and consequences of retrotransposon expression finds activation by BRCA1 in ovarian cancer

Maisa Alkailani[1], Gareth Palidwor[2,3], Ariane Poulin[1], Raghav Mohan[4], David Pepin[4,5], Barbara Vanderhyden[1,6] and Derrick Gibbings[1,*]

[1]Department of Cellular and Molecular Medicine, Faculty of Medicine, University of Ottawa, Ottawa, Ontario, K1H 8M5, Canada, [2]Ottawa Institute for Systems Biology, University of Ottawa, Ottawa, Ontario, K1H 8M5, Canada, [3]Bioinformatics, Ottawa Hospital Research Institute, Ottawa, Ontario, K1H 8L6, Canada, [4]Pediatrics Surgical Research Laboratories, Massachusetts General Hospital, Boston, MA 021145, USA, [5]Department of Surgery, Harvard Medical School, Boston, MA 021156, USA and [6]Cancer Therapeutics Program, Ottawa Hospital Research Institute, Ottawa, Ontario, K1H 8L6, Canada

Received May 03, 2020; Revised November 20, 2020; Editorial Decision November 24, 2020; Accepted November 30, 2020

ABSTRACT

It is challenging to identify the causes and consequences of retrotransposon expression in human disease due to the hundreds of active genomic copies and their poor conservation across species. We profiled genomic insertions of retrotransposons in ovarian cancer. In addition, in ovarian and breast cancer we analyzed RNAs exhibiting Bayesian correlation with retrotransposon RNA to identify causes and consequences of retrotransposon expression. This strategy finds divergent inflammatory responses associated with retrotransposon expression in ovarian and breast cancer and identifies new factors inducing expression of endogenous retrotransposons including anti-viral responses and the common tumor suppressor BRCA1. In cell lines, mouse ovarian epithelial cells and patient-derived tumor spheroids, BRCA1 promotes accumulation of retrotransposon RNA. BRCA1 promotes transcription of active families of retrotransposons and their insertion into the genome. Intriguingly, elevated retrotransposon expression predicts survival in ovarian cancer patients. Retrotransposons are part of a complex regulatory network in ovarian cancer including BRCA1 that contributes to patient survival. The described strategy can be used to identify the regulators and impacts of retrotransposons in various contexts of biology and disease in humans.

INTRODUCTION

Nearly one-half of the human genome is derived from transposable elements (1). Most transposable elements in humans are retrotransposons (1). Transcription of a genomic retrotransposon produces an RNA copy, which is reverse-transcribed and inserted into a new genomic location, in a process termed retrotransposition (2). In humans, there are three major classes of retrotransposons: *Alu,* a primate-specific class of Short-Interspersed Elements, Long INterspersed Element-1 (LINE-1) and Human Endogenous Retroviruses (HERV) (1). A large proportion of retrotransposons are mutated or truncated and incapable of retrotransposition (1). For example, of thousands of LINE-1, only 80–150 copies are highly active (1). Transcription of LINE-1 is usually initiated by RNA polymerase II from an internal promoter within its 5′UTR. This promoter is regulated by DNA methylation of adjacent CpG islands and transcription factors including YY1 and SOX2 (3–5). In the cytoplasm, LINE-1 RNA is translated into ORF1p and ORF2p proteins which associate *in cis* with LINE-1 RNA (1). This ribonucleoprotein complex is imported into the nucleus where LINE-1 is thought to integrate within a new genomic location by target-primed reverse transcription (2). Briefly, ORF2p contains endonuclease activity that produces an ssDNA nick in the target DNA (2). The exposed 3′ sequence anneals to the LINE-1 RNA polyA tail to prime reverse transcription by ORF2p (2). Subsequently, DNA repair processes are presumed to help produce the second DNA strand and repair DNA breaks to finalize genomic insertions of LINE-1, which are frequently truncated at the 5′ end (1).

Alu elements are ∼300 nt and are frequently embedded within introns, 3′UTRs of genes or in intergenic regions (6).

*To whom correspondence should be addressed. Tel: +1 613 562 5800 (Ext 8026); Fax: +1 613 562 5800; Email: gibbings@uottawa.ca

When *Alu* elements are embedded within other transcripts, they are frequently transcribed by RNA polymerase II (6). When transcribed independent of other RNAs, RNA polymerase III transcribes them. *Alu* elements do not encode proteins, but rather hijack LINE-1 ORF1p and ORF2p to mediate their retrotransposition (6).

Transposable elements diverge enormously in type and location between species, and transposable elements account for ∼25% of genetic differences between individual humans (7). *De novo* retrotransposon insertions can occur in exons, introns or regulatory regions of the genome, disrupting their function, or providing new promoter and enhancer regions (8,9). Similarly, the evolutionary drift caused by transposable elements may also occur during tumor evolution (10). In tumors, LINE-1 insertions have been identified in tumor suppressors such as APC (11), ST18 (12) and PTEN (13), suggesting that retrotransposon insertions promote genetic heterogeneity in tumors and at times may instigate tumorigenesis or promote tumor growth (10).

Transcription of RNA from retrotransposons is usually repressed by heterochromatic processes (10), but are induced in stem-cell-like populations (10). This does not always lead to increased rates of retrotransposon insertion, due to cellular defense systems including RNA silencing systems (piRNA) and RNA-DNA nucleases like TREX (10). Retrotransposon intermediates such as the RNA–DNA hybrids formed by reverse-transcription, can also have consequential impacts by inducing release of type I interferons that may drive inflammation in aging, Aicardi-Goutieres syndrome and some tumors (14,15). Induction of retrotransposons in tumors, by treatment with inhibitors of their heterochromatic repression, activates type I interferons and immune responses and promotes tumor elimination (16). Whether constitutive levels of retrotransposons in patient tumors induce type I interferons or they have beneficial impacts remains unclear. Understanding the full range of consequences of retrotransposon expression in tumors and the factors which control their expression is one of the principal areas of current investigation. Identifying the effects of retrotransposons in contexts like human cancer presents challenges because the large number and diversity of genomic copies prevents easy use of research tools such as CRISPR or siRNA to repress them, while over-expression risks inducing non-physiological effects.

To overcome some of these challenges we employed Bayesian correlation analysis of retrotransposon expression using RNA sequencing data from The Cancer Genome Atlas (TCGA) alongside analysis of *de novo* LINE-1 insertions. This permitted identification of multiple factors controlling and induced by retrotransposon including BRCA1 and suggested that retrotransposon expression is associated with survival of ovarian cancer patients independent of effects on type I interferons and immune responses.

MATERIALS AND METHODS

Reverse transcriptase-quantitative polymerase chain reaction (RT-qPCR) was performed after RNA isolation from cells using TRIzol (Invitrogen). RNA samples were DNaseI (Qiagen, 79254) treated in Figures 2, 3 and 6. cDNA was prepared in Figures 4 and 5 using Oligo(dT) and dNTPs with M-Mulv RT (NEB#M0253) and in Figures 2, 3 and 6; Supplementary Figures S4 and 5 using MiScript II Reverse Transcriptase system (Qiagen). GoTaq qPCR Master Mix (Promega A6002) was used for qPCR with primers specific to human or mouse as listed in the Supplementary Table S3. Relative quantities were calculated using the $\Delta\Delta C$t method, normalized to the geometric mean of β-actin and GAPDH unless otherwise indicated.

Cells and reagents

HeLa (CCL2, ATCC), HEK 293T cells (CRL-3216, ATCC) were cultured in Dulbecco's-modified Eagle's medium containing 10% fetal bovine serum and 2 mM L-glutamine. ES2 and MOSE cells (from Dr Barbara Vanderhyden) were cultured in Modified McCoy's 5a Medium with 10% fetal bovine serum and 'MOSE medium' as described in (17), respectively. Lipofectamine 2000 (Invitrogen) was used to transfect Poly I: C (R&D, 4287/10) or the following plasmids into cells: pEGFP-N1 (a gift from S. Pfeffer, Strasbourg), 99 RPS-GFP PUR, 99 RPS-GFP JM111 PUR, pCEP 5′UTR ORF2 no-Neo, *Alu*-neo^{Tet}, pcDNA3.1, and HA-ORF1 (gifts from J. Goodier), L1-neo-TET (18) (Addgene # 51284). Silencer Select siRNAs (Life Technologies, Supplementary Table S4) were transfected using RNAiMax at a concentration of 10 nM (Life Technologies).

Western blotting

After lysis (RIPA buffer) proteins were resolved on 8% (w/v) acrylamide gels, transferred to PDVF membrane (IPVH00010, EMD Millipore), blocked with 5% milk in TBST (1 h) and probed with primary antibody in TBST overnight at 4°C. The primary antibodies (Supplementary Table S5) were detected with anti-IgG-HRP and HRP substrate (WBLUR0100A, EMD Millipore) using ImageQuant LAS 4000 system (GE Healthcare). Quantification of blots was performed using total intensity of an area encompassing the maximum band size using the Image Studio Lite Ver 5.2 software (LI-COR Biosciences) and normalized to Tubulin after subtracting background.

Cancer spheroid *in vitro* cultures

A panel of primary ovarian cancer cell lines, derived from ascites of patients with high-grade serous histology (IRB-approved protocol #2007P001918/MGH), with confirmed BRCA1 mutations ($N = 4$) or wild-type ($N = 4$) status by clinical SNaPshot™ genotyping, was used. Briefly, low-passage primary cancer cells were grown in RPMI1640 (Gibco) with B27 supplement (Life Technologies), penicillin/streptomycin (Life Technologies), without any serum additives as previously described (19).

LINE-1 retrotransposition assay

LINE-1 assay was performed as previous (20) with modifications described briefly in Supplementary Methods.

Alu retrotransposition colony formation assay

Alu assay was performed as previous (20) with modifications described briefly in Supplementary Methods.

Northern blot

A protocol for Northern blot detection of LINE-1 previously described (21) was followed with the following modifications. RNA from ES2 cells was treated with DNase I (Qiagen, 79254) and diluted in loading buffer. RNA samples were heated at 70°C for 10 min and run on a 1% formaldehyde agarose gel. RNA was capillary transferred (22) to Nylon membrane (Roche, 11417240001) overnight in 6× Saline Sodium Citrate (SSC) buffer at room temperature. RNA was crosslinked to the membrane with 120 mJ UV using a Stratalinker 2400. Membrane was pre-hybridized for 30 min at 42°C in 30% formamide, 1X Denhardt's solution, 1% sodium dodecyl sulphate, 1 mM NaCl and 1 μl/ml salmon sperm DNA and RNase free water.

Probes specific for L1HS were generated using two approaches. First, twelve 21–23 nt oligonucleotides were designed to recognize the 900 nt 5′ end of L1HS specifically at regions absent from L1PA or with sequence differences compared to L1PA. As a loading control 12 short oligonucleotides complementary to *GAPDH* mRNA were used. Probes recognizing L1HS or *GAPDH* were pooled and labeled with ^{32}Pγ-ATP as described (23). All sequences are in Supplementary Table S7.

As an alternative, L1HS was detected using a probe recognizing the 486 nt in the 5′UTR of L1HS. Probe DNA was amplified from HEK293T DNA by PCR using Taq DNA polymerase (BioBasic) using primer pairs 5′-gggaggaggagccaagat and 5′-ccggctgctttgtttaccta for L1HS; and 5′-accacagtccatgccatcac and 5′-gcttgacaaagtggtcgttg for GAPDH, respectively. PCR products were gel-purified using the Qiagen PCR cleanup kit. Radiolabeled probes were generated as described (24). Briefly, 25 ng of clean PCR product in 30 μl water with 125 ng random hexamer deoxynucleotide primers (IDTDNA) was heated for 2 min in a boiling water bath and snapped cold on ice. dATP, dGTP and dTTP (Applied Biosystems, 250 μM final concentration) were added to 10 μl of 5× random priming buffer (250 mM Tris–Cl pH8.0, 25 mM MgCl2, 100 mM NaCl, 10 mM Dithiothreitol, 1 M HEPES pH 6.6), 5 μl [α-32P] dCTP (10 mCi/ml, 3000 Ci/nmol; Perkin Elmer) and the reaction brought to 50 μl with water. Five U of Klenow DNA polymerase (NEB) were added (60 min, room temperature) and the reaction was terminated with 10 μl stop buffer (50 mM Tris–Cl pH 7.5, 50 mM NaCl, 5 mM EDTA, 0.5% w/v SDS). Labeled probe heat denatured before use in northern blots. Probes were incubated with rotating membranes overnight at 42°C. Membranes were washed twice in 5× SSC and once in 1× SSC.

Co-immunoprecipitation (Co-IP) and RNA immunoprecipitation (RIP)

Cells were washed in cold phosphate-buffered saline, lysed and scraped in RIPA lysis buffer or RNA immunoprecipitation (RIP) lysis buffer. Cell lysate was incubated inverting for 20 min at 4°C and centrifuged at 1000 × *g*, 5 min to exclude insoluble materials. Supernatant was incubated inverting 20 min at 4°C with 10 μl of pre-washed protein G-Dynabeads to pre-clear. Beads were removed using a magnetic support (12321D, Thermo Fisher Scientific) and supernatant protein content was measured. Equal amounts of protein mass were incubated with equal amounts of antibody of interest and its corresponding nonspecific IgG control antibody for 3–4 h at 4°C. A total of 20 μl wet volume of protein G-Dynabeads were added to each IP for a further 1 h at 4°C. Beads were collected and washed with 200 μl RIPA buffer or RIP wash buffer three times at least. Co-IPs samples were processed for western blot analysis and RIP samples were TRIzol (Invitrogen) RNA isolated as in the manufacturers' protocol.

Chromatin immunoprecipitation (ChIP) and DNA–RNA immunoprecipitation (DRIP)

Protocol for chromatin immunoprecipitation (ChIP) (25) and DNA–RNA immunoprecipitation (26) was followed with minor modifications described in Supplementary Data.

Pulse labeling of RNA with ethynyl uridine

Pulse labeling was performed using the Nascent RNA Click-iT kit (Life Technologies) according to the manufacturer's instructions. Briefly, cells were plated at 2.5 × 10^5 per well in a 6-well plate and transfected with siRNA the following day. Seventy-two hours after transfection, ethynyl uridine (0.2 mM) was added. Media was changed after 1 h incubation and RNA was extracted 1 h later using TRIzol (Invitrogen). RNA (5 μg) was labeled with biotin (0.5 mM Biotin Azide per sample). Pulse-labeled, biotinylated RNA (500 ng) was captured using Dynabeads Streptavidin T1 magnetic beads and used as a template for cDNA synthesis using MiScript II Reverse Transcriptase system (Qiagen).

Statistical analysis

Two-tailed t-test, and two-way ANOVA were employed to evaluate the statistical significance of experiments where appropriate in GraphPad Prism software on a minimum of three independent biological replicates. A *P*-value of <0.05 was considered statistically significant. Significance was denoted as follows: **P*-value < 0.05, ***P*-value < 0.01, ****P*-value < 0.001, *****P*-value < 0.0001.

Bioinformatics, retrotransposon insertions, RNA levels and methylation

Detailed methods are available in the Supplementary Data.

RESULTS

To assess retrotransposon insertions in tumors of patients with serous ovarian adenocarcinoma we used The Mobile Element Locator Tool (MELT) (27). This tool uses genome sequencing reads which span the junction between a retrotransposon and the reference genome to map the sites of retrotransposon insertions. Genome sequencing data from TCGA with matched normal and ovarian tumor samples was available from 54 patients with >20× coverage that approaches saturation in identifying retrotransposon insertions using MELT (Supplementary Figure S1A). Retrotransposon insertions catalogued in other genomes by the

European database of L1-HS retrotransposon insertions (EUL1Db) (28,29), and therefore likely inherited, were eliminated. Retrotransposon insertions in regions with frequent mapping errors were also eliminated, leaving 1813 LINE-1 insertions. Insertions found in both tumor and normal tissues (1,121), were eliminated as germline insertions specific to the patient or restricted populations. The 692 remaining insertions were considered to be tumor-specific. Ovarian tumors exhibited a range of 0 to 64 *de novo* tumor-specific LINE-1 insertions (Figure 1A and Supplementary Table S1A). While most ovarian tumors had an evenly distributed range of between 0 and 30 tumor-specific LINE-1 insertions, three patients exhibited much higher numbers of LINE-1 insertions (40–64, Figure 1A). The number of patient-specific LINE-1 insertions in normal tissue was far higher than in tumors and did not correlate with the number of LINE-1 insertions in tumors (Figure 1B and Supplementary Table S1A). This suggests that the number of tumor-specific LINE-1 insertions is minimal compared to those likely inherited in rare populations or accumulated over the patient's lifetime.

LINE-1 insertions rarely impact tumor suppressors or oncogenes in ovarian cancer

LINE-1 insertions in ovarian tumors distributed broadly over chromosomes (Figure 1C and Supplementary Dataset 1), but clusters of insertions were observed, even after excluding those in repetitive sequences prone to mapping artefacts (e.g. microsatellites) within a sliding 500 bp window as potential errors in mapping insertion sites. The highest density of novel LINE-1 insertions in ovarian cancer was in a region encoding MHC class II HLA-DR (Supplementary Figure S1B), with other insertions clustered on chromosome 20 (neighborhood of LINC01597) and chromosome 3 (neighborhood of EPHA3) among others (Supplementary Table S1B and Dataset 1). This suggests that LINE-1 may have a propensity to insert in certain genomic regions. Alternatively, insertions in regions, such as HLA-DR and EPHA3, which have been associated with ovarian cancer growth (30,31), may provide a competitive advantage selected during tumor evolution.

Of 692 LINE-1 insertions in ovarian cancer genomes, 30 disrupted exons of protein-coding genes (Supplementary Table S1B), a rate of gene-disruption significantly greater than random chance (30/692 insertions = 4.3% in exons, 1.1% of genome contains exons, $P > 0.001$ Fisher's test) in agreement with previous research. There was no enrichment for insertions in genes that were previously (32) found to be essential for or promote proliferation (Figure 1D). Two *de novo* LINE-1 insertions interrupted the putative oncogenes MMS22L and BCL11A and putative tumor suppressors ARHGEF12 and NEBL (33). This suggests that LINE-1 insertions in tumor suppressors may in rare cases exert selective pressure in ovarian cancers, but that in general new LINE-1 insertions in ovarian cancer only infrequently and randomly disrupt tumor suppressors, oncogenes or essential genes by interrupting their coding regions.

New tumor-specific LINE-1 insertions could also impact tumor progression by altering DNA methylation, or acting as promoters, enhancers or inhibitors of expression of proximal genes. Genes proximal to tumor-specific LINE-1 insertions (±10 kb) tended to have lower RNA expression and DNA methylation (Figure 1C and Supplementary Dataset 2). In a small number of cases new LINE-1 insertions were observed proximal to genes frequently mutated in cancer (BAZ1A, WT1) or a probable tumor suppressor in ovarian cancer (VGLL3), however among these genes, only levels of VGLL3 mRNA ranked in the lower percentiles (Supplementary Dataset 2). This suggests that in rare cases new insertions of LINE-1 can impact expression of tumor promoting genes.

Together, the presented evidence suggests that in most cases of ovarian cancer new LINE-1 insertions have minimal impact on tumorigenesis or tumor progression. While the three patients with unusually high numbers of tumor-specific LINE-1 insertions succumbed early to disease, in general there was no correlation between number of LINE-1 insertions and patient survival in ovarian cancer (Figure 1E).

Levels of retrotransposon RNA predict survival of ovarian, but not breast cancer patients

LINE-1 insertions in the genome did not consistently impact patient survival, but recent studies demonstrated that chemically induced over-expression of retrotransposons and their RNA–DNA intermediates in animal models of cancer can be immunogenic and generate tumor repressive effects (15,16). We sought to use patient data to assess whether levels of retrotransposon RNA habitually found in patient tumors is sufficient, among tumor heterogeneity, to measurably impact patient survival. We therefore analyzed retrotransposon RNAs in ovarian serous adenocarcinoma or invasive breast carcinoma tumors using data from TCGA. Retrotransposon RNAs were mapped to Repbase (34,35) and quantified using Repenrich (36) using RNA sequencing data from 379 and 486 patients (ovarian cancer and breast cancer, respectively). To focus on more intact retrotransposition-competent RNAs we analyzed younger LINE-1 (L1PA), *AluY* and HERVK families. Levels of tumor-specific LINE-1 insertions correlated poorly with levels of LINE-1 RNA (Supplementary Figure S2A).

Ovarian cancer patients whose ovarian tumors exhibited LINE-1 expression in the highest quartile exhibited better survival than those with LINE-1 expression in the lowest quartile (Figure 2A and Supplementary Figure S2B). A similar analysis performed using RNA expression data from breast cancer tumors, found no correlation with survival in this cancer (Figure 2B). Differences in tumor grade, size or invasion did not account for the difference in survival between ovarian cancer patients with top quartile LINE-1 expression (Supplementary Figure S2C–F). This suggests that factors induced by retrotransposons or co-regulated with them promote survival of ovarian, but not breast cancer patients.

A strategy to survey the causes and consequences of retrotransposon RNA production in cancer

We sought to broadly survey the impact of retrotransposon RNA in ovarian and breast cancers and the mechanisms controlling their expression. Heterochromatin and

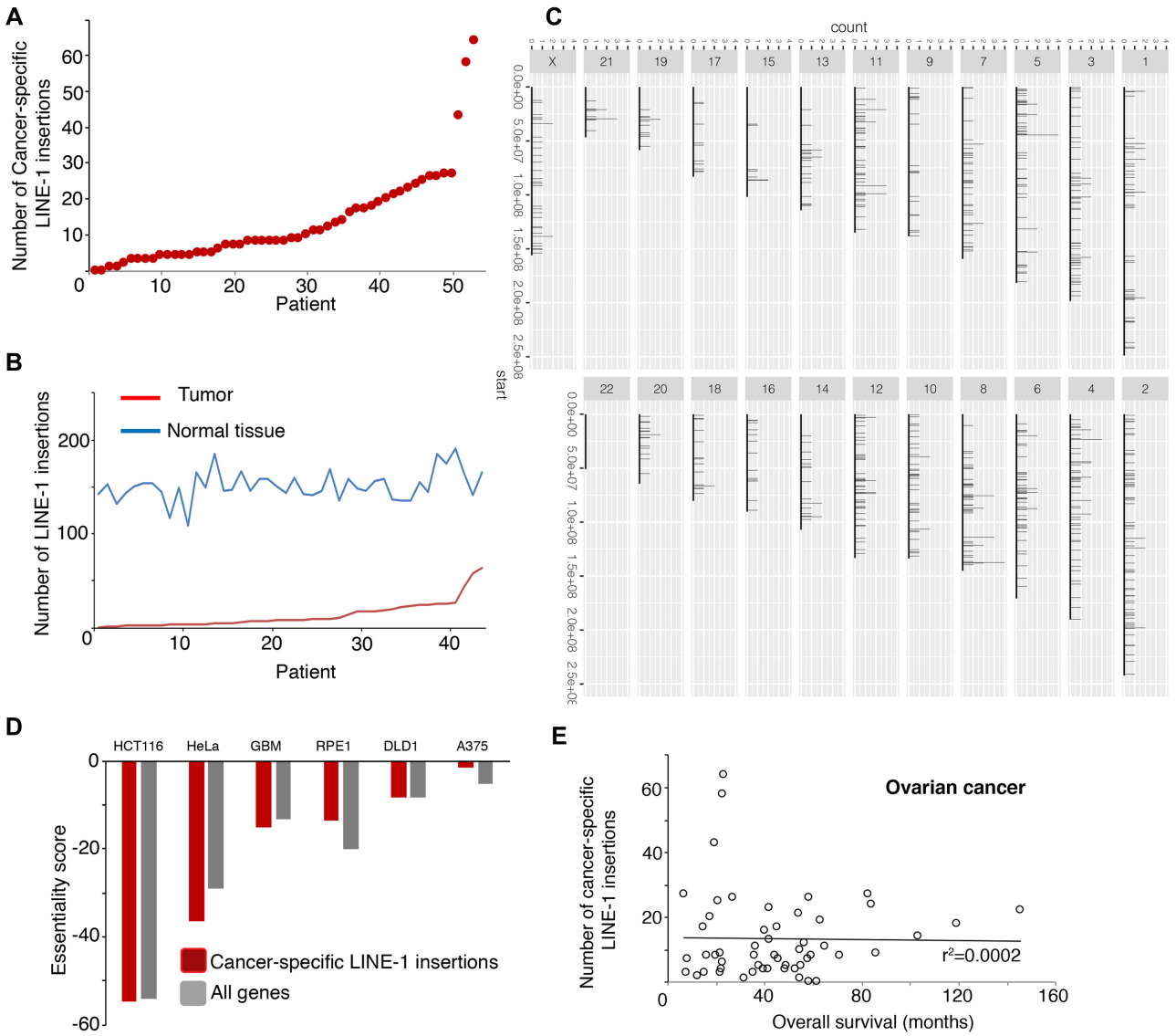

Figure 1. *De novo* insertions of LINE-1 in ovarian cancer. (**A**) Number of *de novo* tumor-specific LINE-1 insertions (*y*-axis) in each of 54 patients (*x*-axis). (**B**) Number of *de novo* LINE-1 insertions (*y*-axis) in either normal tissue samples or tumor samples from each patient (*x*-axis). (**C**) Plot of *de novo* LINE-1 insertions in tumor samples across 22 chromosomes after elimination of putative insertions in blacklisted regions identified as difficult to map by ENCODE. Peak height indicates count of LINE-1 insertions. (**D**) Essentiality score (32) for cancer specific LINE-1 insertions versus all genes in the indicated cell lines (*x*-axis). (**E**) Correlation plot of LINE-1 genomic insertions versus patient survival.

DNA methylation can control retrotransposon expression (16,37); however global DNA methylation did not correlate with retrotransposon levels (Figure 2C and Supplementary Figure S3A). We used Bayesian correlation to identify RNAs whose expression correlated with each retrotransposon class (LINE-1, *AluY*, Figure 2D and Supplementary Table S2A). This analysis uses sequences that match young, retrotransposition-competent elements, however it cannot exclude retrotransposons embedded within other transcripts, or other chimeric RNAs containing retrotransposon sequences that may affect results. Correlated RNAs will include many RNAs which are indirectly co-regulated with retrotransposons, however they will also include a proportion encoding proteins that directly control expression of retrotransposons, or that are induced by retrotransposons.

Retrotransposon RNA is induced by and induces type I interferon responses

We first assessed RNAs which correlated with levels of retrotransposon RNAs to identify candidate RNAs previously reported to be induced by retrotransposons in cancer. Retrotransposons can induce type I interferons and promote apoptosis and immunogenic responses in tumors and other tissues (16,37). A previous report described immune responses associated with retrotransposon expression which correlated with expression of Toll-receptors, immunoregulatory molecules and some mRNAs whose transcription is activated by interferon (38). These mRNAs generally exhibited only weak associations ($r < 0.2$) with retrotransposon expression in breast and ovarian cancer (Supplementary Table S2C). Among RNAs highly corre-

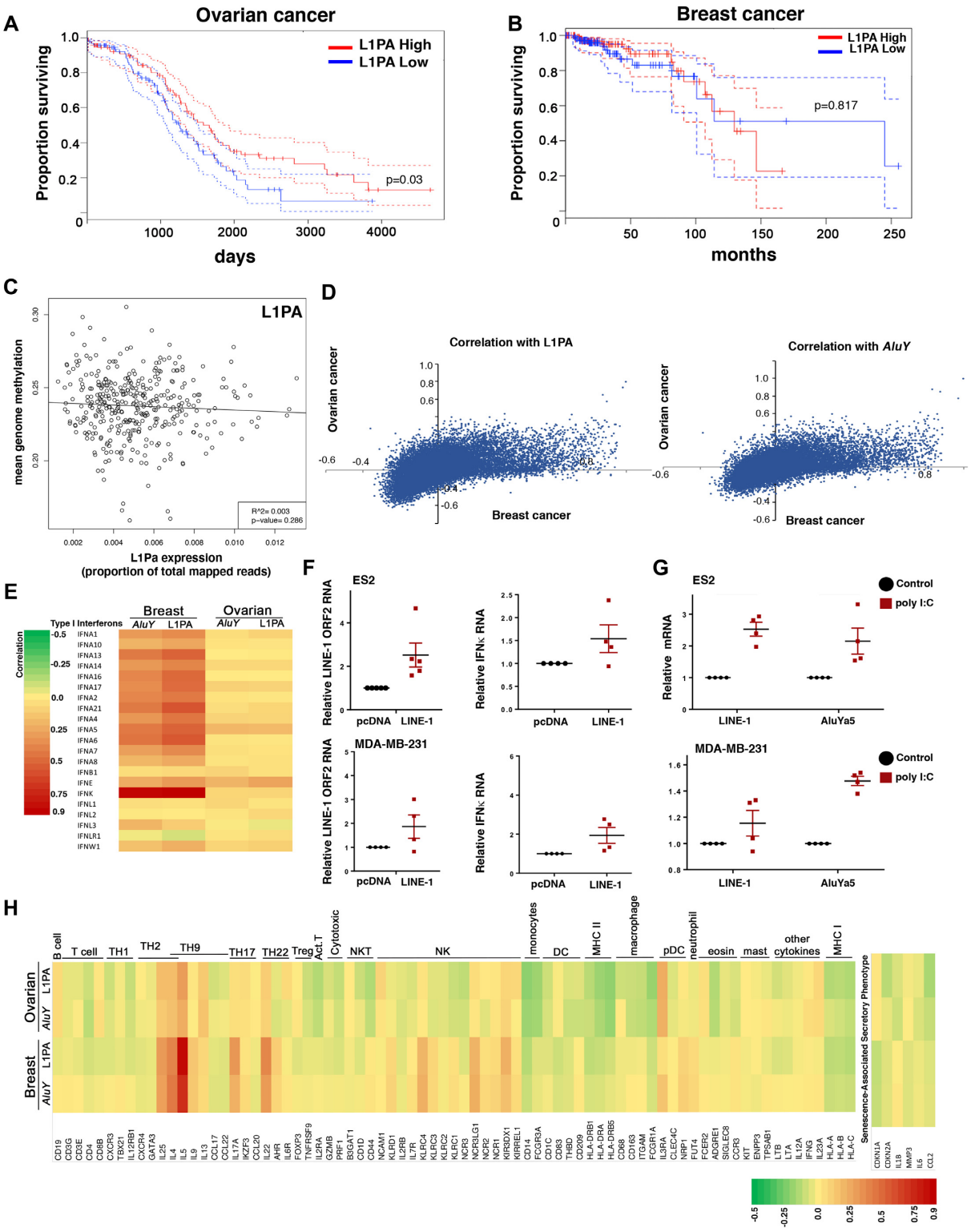

Figure 2. LINE-1 RNA predicts survival of ovarian cancer patients and retrotransposon expression correlations with DNA methylation and inflammatory mediators. (**A** and **B**) Kaplan–Meier survival plots of ovarian (A) or breast (B) cancer patients with top or bottom quartile expression of LINE-1 PA RNA. Solid lines indicate average and broken lines indicate confidence interval. Error bars in all graphs represent standard error of the mean. (**C**) Correlation of LINE-1 RNA expression (proportion of total reads mapped) with mean genome methylation in ovarian cancer. (**D**) Plot of Bayesian correlation values of each gene with LINE-1 (left) or *AluY* (right) expression in ovarian cancer versus in breast cancer. (**E**) Heat map of Bayesian correlation values of type I interferons with LINE-1 or *AluY* RNA in ovarian and breast cancer. (**F**) RT-qPCR of LINE-1 ORF2 or IFNK mRNA after transfection of ES2 or MDA-MB-231 cells with LINE-1 expressing plasmid versus control plasmid. $N = 4$–5 independent biological replicates. (**G**) RT-qPCR of LINE-1 (ORF2) or *AluY* RNA after transfection of ES2 or MDA-MB-231 cells with the activator of anti-viral responses poly I:C (1μ g/ml). $N = 4$ independent biological replicates. (**H**) Heat map of Bayesian correlation values of immunological responses or the senescence associated secretory phenotype with LINE-1 or *AluY* RNA in ovarian and breast cancer. In RT-qPCR horizontal lines represent averages and error bars indicate standard error of the mean.

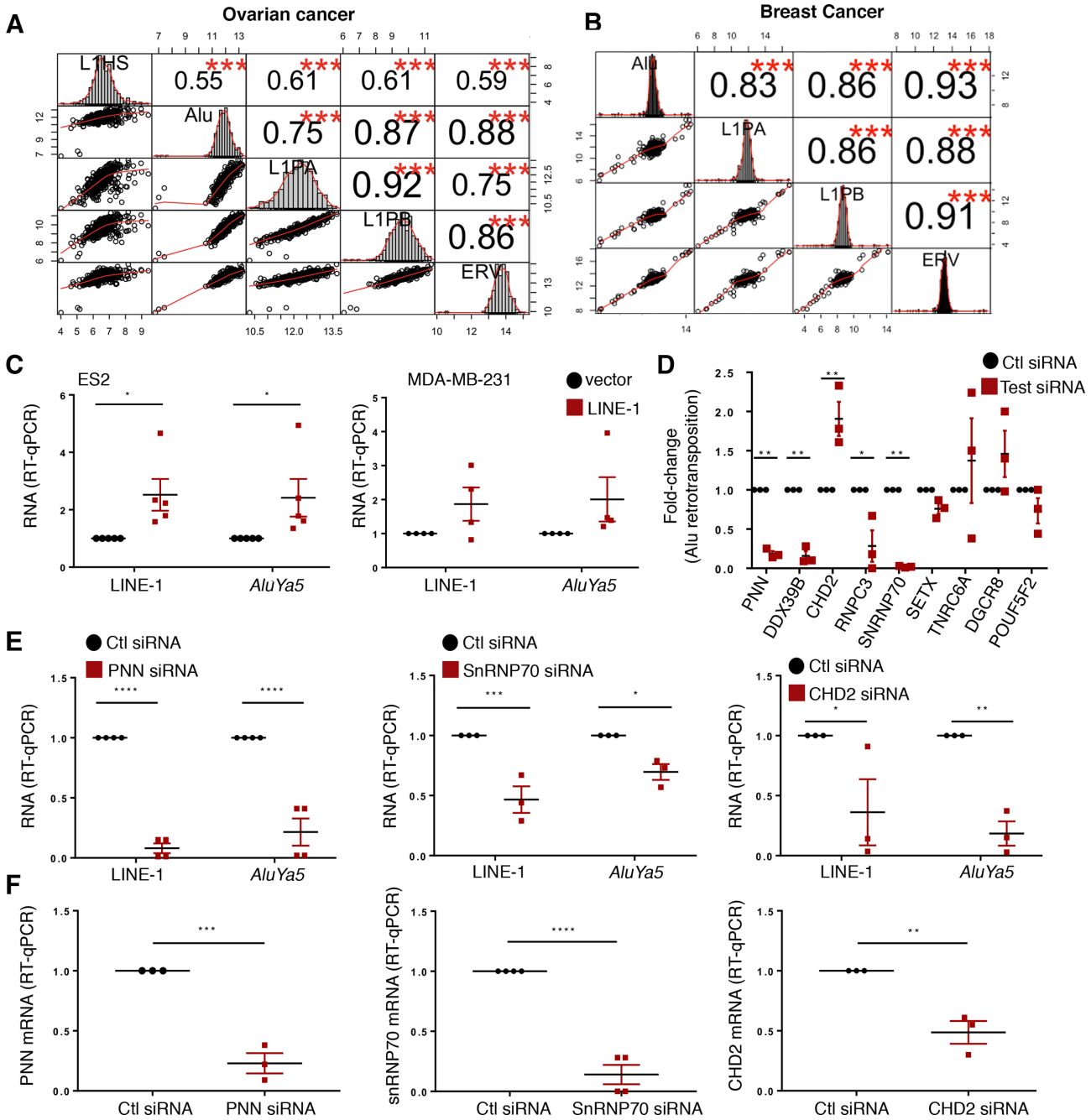

Figure 3. Bayesian Correlation Predicts Genes Regulated by or Induced by Retrotransposons. (**A** and **B**) Pearson correlation (r) of LINE-1 families, *AluY*, and HERVK RNA (proportion of total reads mapped) in ovarian cancer (A) and breast cancer (B). Dot plots represent correlation of mean expression values per patient. Histograms represent distribution of expression of indicated retrotransposons. Numbers indicate the *r* correlation value. (**C**) RT-qPCR of LINE-1 (ORF2) and *AluYa5* retrotransposon RNA two days after transfection with plasmid expressing LINE-1. $N = 4$–5 independent biological replicates. Data on LINE-1 RNA levels is also used in Figure 2F. (**D**) *Alu* retrotransposition assay fold-change in colony numbers after transfecting cells with control siRNA or siRNA targeting the indicated test gene. (**E**) RT-qPCR of LINE-1 (ORF2) and *AluYa5* retrotransposon RNA two days after transfection with indicated siRNA. $N = 3$–4 independent biological replicates. (**F**) RT-qPCR of the target of the siRNA performed in the samples used in (E) to validate target knockdown. $N = 3$–4 independent biological replicates. In RT-qPCR horizontal lines represent averages and error bars indicate standard error of the mean. *$P < 0.05$, **$P < 0.01$, ***$P < 0.001$, ****$P < 0.0001$ two-way ANOVA with Holmes-Sidak correction (C–E) *t*-test (F).

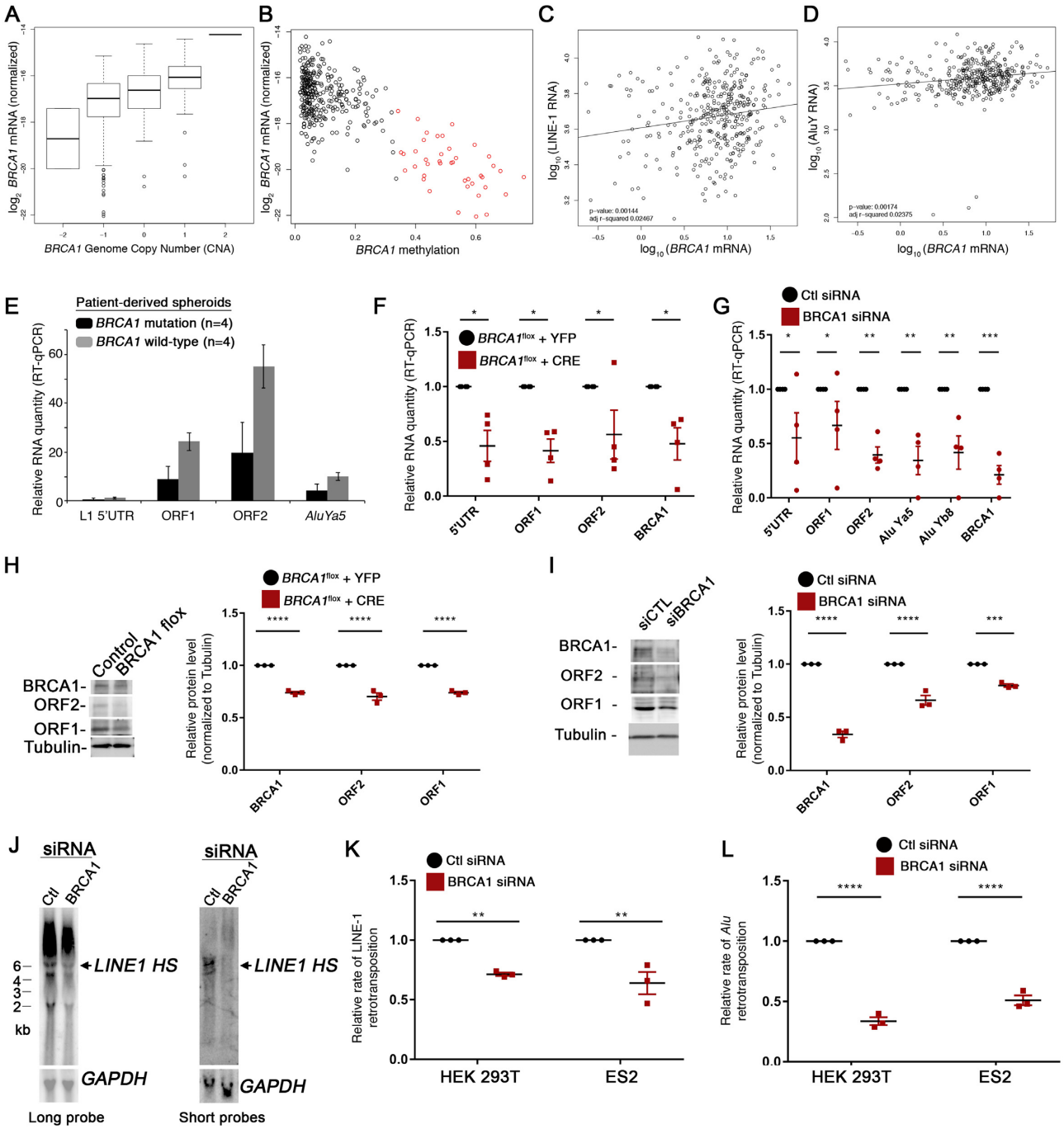

Figure 4. BRCA1 Controls Levels of LINE-1 and *AluY* and their retrotransposition. (**A**) Graph of BRCA1 mRNA levels obtained by RNaseq in tumor samples from The Cancer Genome Atlas (TCGA) grouped based on the copy number of *BRCA1*. (**B**) Correlation plot of BRCA1 mRNA levels versus methylation scores for *BRCA1* in tumor samples from TCGA. Samples with high levels of *BRCA1* gene methylation are colored in red. (**C** and **D**) Correlation plot of LINE-1 (C) and *AluY* (D) RNA levels (proportion of total mapped reads) versus BRCA1 mRNA levels in tumor samples from TCGA. (**E**) RT-qPCR of LINE-1 and *AluY* RNA levels in spheroid cultures generated from patient tumors ascites either with or without *BRCA1* loss or mutations. Error bars represent standard error of the mean. (**F** and **G**) RT-qPCR of retrotransposon RNA levels in (F) mouse primary ovarian epithelial cells wild-type or with loss of one copy of *BRCA1* (Cre-lox) and (**G**) ES2 cells transfected with siRNA targeting BRCA1. (**H** and **I**) Western blot of LINE-1 ORF1 and ORF2 proteins in (H) mouse primary ovarian epithelial cells wild-type or with loss of one copy of *BRCA1* (Cre-lox) and (I) ES2 cells transfected with siRNA targeting BRCA1. Right, quantification of LINE-1 protein levels by western blots $N = 3$ independent biological replicates. (**J**) Northern blot of LINE-1 in RNA from cells treated with siRNA targeting BRCA1 or control. Blots were probed with either a long probe synthesized with ^{32}CTP that recognizes the 5′UTR of L1HS, or with 12 short ^{32}ATP-labeled probes designed to distinguish L1HS from other L1PA family members. GAPDH was probed as a loading control. (**K** and **L**) Relative rate of (K) LINE-1 or (L) *Alu* retrotranspositions in cells after treatment with control or BRCA1 siRNA. In all graphs, horizontal lines represent averages and error bars represent standard error of the mean. *$P < 0.05$, **$P < 0.01$, ***$P < 0.001$, ****$P < 0.0001$ two-way ANOVA with Holmes-Sidak correction.

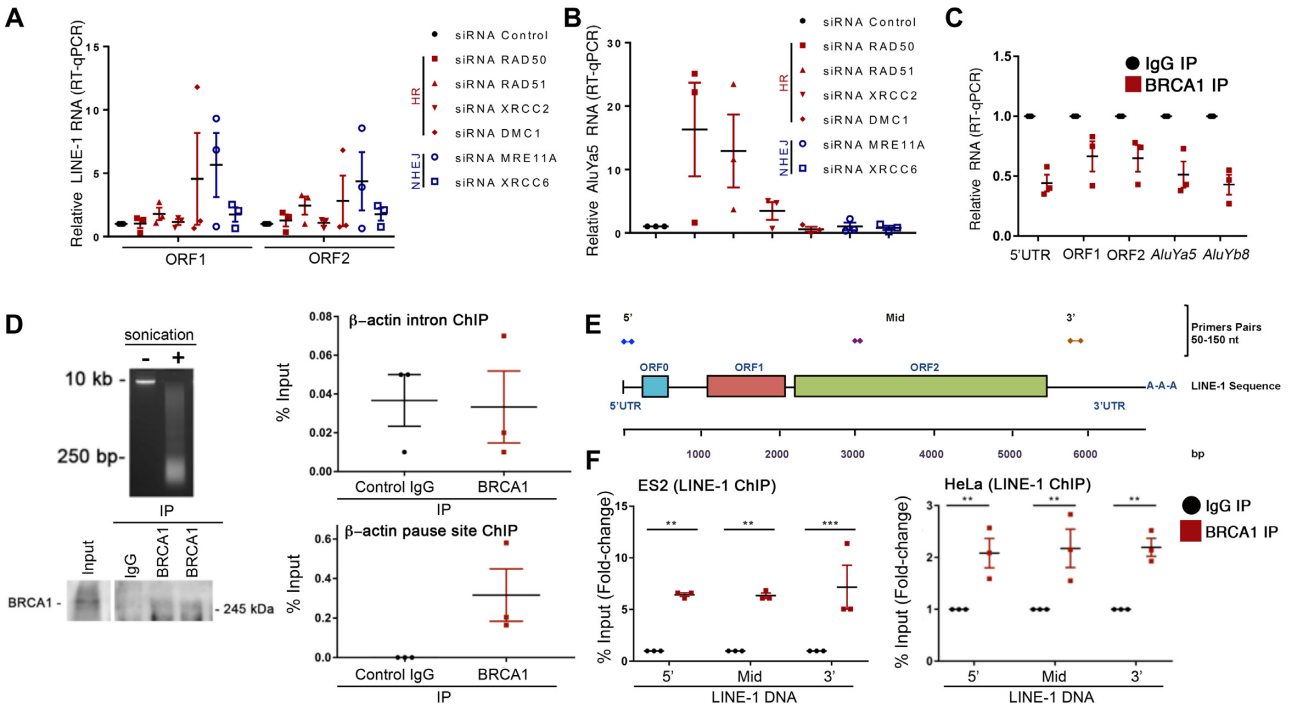

Figure 5. BRCA1 associates with DNA copies of LINE-1 but affects retrotransposition independent of DNA damage repair. (**A** and **B**) RT-qPCR of LINE-1 (A) and *AluYa5* RNA (B) two days after transfection of cells with siRNA targeting the indicated genes involved in DNA damage repair. (**C**) RT-qPCR for the indicated retrotransposon RNAs in BRCA1 IP versus IgG control IP. (**D**) BRCA1 ChIP. Top left, chromatin is disrupted by sonication into ∼200 bp fragments as expected. Bottom left, western blot of BRCA1 immunoprecipitates versus IgG control immunoprecipitates. Right, qPCR results of BRCA1 ChIP for genomic sites bound by BRCA1 (β-actin pause site) or not (β-actin intron) expressed as percent of input sonicated DNA. (**E**) Diagram indicating placement of primers in 5′UTR, mid-region or 3′UTR of LINE-1 for BRCA1 ChIP. (**F**) Quantitative PCR for LINE-1 genomic regions normalized to percent input. In all graphs, horizontal lines represent averages and error bars represent standard error of the mean. $*P < 0.05$, $**P < 0.01$, $***P < 0.001$ two-way ANOVA with Holmes-Sidak correction except (D) where a *t*-test was used.

lated with retrotransposon RNAs ($r > 0.4$) in breast cancer were a large number of type I interferons including many paralogous IFNα mRNAs (IFNA21, IFNA6, IFNA13, IFNA5, IFNA16 etc., Figure 2E and Supplementary Table S2A). Notably, the type I interferon IFNκ was correlated at $r > 0.87$ with retrotransposons in breast cancer. In contrast, in ovarian cancer all type I interferons with the exception of IFNε and IFNA5 ($r < 0.27$) exhibited very poor correlations ($r < 0.1$) with retrotransposon RNAs (Figure 2E). To test whether retrotransposon expression induces type I interferons we expressed LINE-1 RNA in ovarian and breast cancer cell lines (ES2 and MDA-MB-231). Modest increases in LINE-1 RNA enhanced IFNκ mRNA expression in both ES2 and MDA-231 cells (Figure 2F). Intriguingly, activation of type I interferon responses by transfecting cells with poly I:C also induced LINE-1 and *AluY* RNA expression (Figure 2G). This suggests that type I interferons are both produced in response to LINE-1 expression and activate further LINE-1 expression in a self-amplifying loop that is apparent in breast cancer but attenuated in ovarian cancer. Despite the high levels of type I interferon in breast cancer tumors with high levels of LINE-1 RNA (Figure 2E), LINE-1 expression had no impact on survival of breast cancer patients (Figure 2B). This suggests that despite high levels of type I Interferon likely induced by retrotransposon RNA in breast cancer, this is insufficient to impact patient survival. The effect of L1 expression on survival of ovarian cancer patients is independent of type I interferon responses.

Retrotransposons may also activate immune responses more broadly and recruit immune cells into the tumor (38). Cell-type-specific RNAs can serve as a measure of the abundance of specific cell types in whole tissue analysis (39). We applied this method to identify cytokines and immune cells infiltrating tumors containing abundant retrotransposon RNA. Markers of cytotoxic T cells, monocytes and antigen-presenting cells were all negatively correlated with retrotransposon RNA in ovarian cancer and to a lesser extent in breast cancer (Figure 2H). Intriguingly, IL-25 stimulates production of Th2 cytokines like IL-4, IL-5 and IL-13 (40), all of which exhibited the strongest positive correlations with retrotransposon RNAs of any analyzed cytokines in both breast and ovarian cancer (Figure 2H). Retrotransposon RNAs were not associated with inflammatory markers of a secretory-associated senescent response that is associated with retrotransposon activation in aging (15) (Figure 2H). This suggests that retrotransposon RNA is predominantly associated with a Th2 and Th9-type immune profile. While the cause of this is uncertain, it may be a symptom of the ability of tumor cells with abundant retrotransposon RNA to avoid killing in a Th2 environment that represses cytotoxic responses.

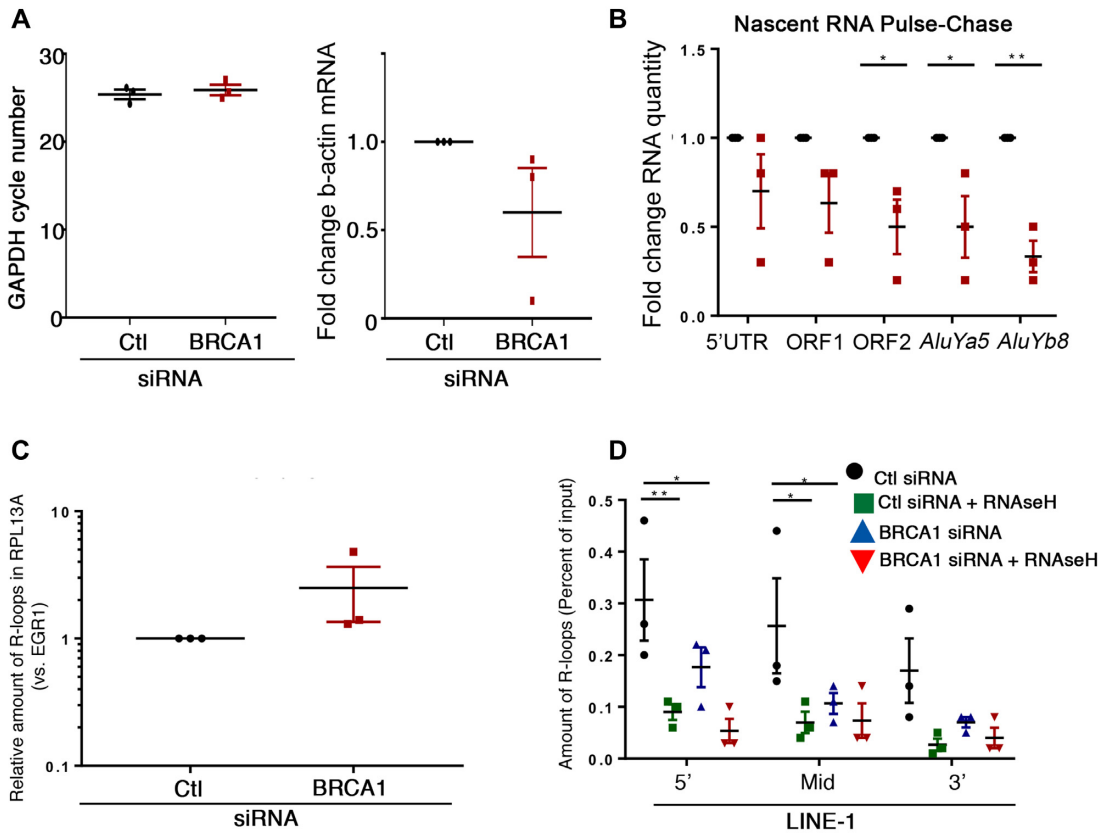

Figure 6. BRCA1 promotes transcription of retrotranposon RNA. (**A** and **B**) Nascent RNA pulse-chase analysis in ES2 cells. RT-qPCR of GAPDH crossing threshold cycle number (left) and fold-change in β-actin mRNA levels (versus GAPDH) (A), and LINE-1 and *AluY* RNAs among purified nascent RNAs 1 h after pulse of cells with ethynyl-uridine (B). (**C** and **D**) RT-qPCR of R-loops purified with S9.6 antibody from cells transfected with control or BRCA1 siRNA. (C) R-loop enrichment is expressed as quantitative PCR values for primers at RPL13A versus values for a site with few R-loops (EGR1). (D) quantitative PCR of R-loops enrichment at LINE-1 in cells transfected with siRNA targeting BRCA1 or control, and S9.6 immunoprecipitates treated or not with RNase H to degrade RNA-DNA hybrids. In all graphs, horizontal lines represent averages and error bars represent standard error of the mean. $^{*}P < 0.05$, $^{**}P < 0.01$ two-way ANOVA with Holmes-Sidak correction except for (A and C) where a *t*-test was used.

A subset of RNAs correlated with retrotransposons promote their expression

The analysis of type I interferons suggests that Bayesian correlation has predictive power to identify RNAs controlling retrotransposon expression or induced by them. We aimed to identify new factors regulating and induced by retrotransposons using this approach. Remarkably, levels of LINE-1, *AluY* and HERVK RNAs correlated more closely with each other in all combinations ($r = 0.55$ to $r = 0.93$) than with any other mRNA in both ovarian cancer and breast cancer (Figure 3A and B). RNA derived from LINE-1 elements with the most retrotransposition activity (L1HS) also correlated closely with expression of other retrotransposons including the broader L1PA family (Figure 3A and B). In general, mRNAs correlated similarly with broader L1PA family and the more active L1HS family (Supplementary Table S2B). Over-expression of LINE-1 augmented the level of *AluY* RNA (Figure 3C), potentially due to stabilization of *AluY* RNA when it binds to LINE-1 ORF1 protein. Additional tumor properties which act on pathways affecting all retrotransposon classes, such as those controlling transcription, epigenetics or RNA stability may contribute to their tight correlation among retrotransposon classes in these cancers.

Genes correlated with LINE-1 expression in ovarian cancer were highly enriched in binding sites for the YY1 and Oct1 transcription factors (Supplementary Table S2D). In breast cancer Oct/Pou family, MEF2C family, and SATB1 binding sites were enriched in genes co-regulated with retrotransposon RNA (Supplementary Table S2D). YY1 binding sites in the 5′UTR promoter of LINE-1 elements have previously been shown to control LINE-1 expression (4), Oct2 binds to LINE-1 elements (41) and SATB1 binds *Alu* sites in the genome (42). This suggests that YY1 and SATB1 activity may control a gene expression program including retrotransposon induction in ovarian and breast cancer respectively.

The interactome and GO-terms (43,44) of RNAs highly correlated with retrotransposon expression were assessed to identify additional candidate processes or complexes, which govern retrotransposon RNA levels. Among 378 RNAs correlated $r > 0.6$ with L1PA in breast cancer a concentration of Histones and G protein-coupled receptors was detected by GO-term analysis (45) (Supplementary Table S2E). Among 233 RNAs correlated with L1PA in ovarian cancer ($r > 0.4$), GO-terms were enriched for RNA processing, RNA splicing, RNA metabolism and mitochondrial function among others (Supplementary Table S2E). Net-

works of interacting RNA binding proteins were apparent among these (Supplementary Figure S3B). Notably TDP-43 which multiple papers have demonstrated to control retrotransposon activity (46–48), exhibited the strongest negative correlation with retrotransposon RNAs in breast cancer.

We sought to identify RNA features of ovarian cancer with maximum predictive power for expression of retrotransposons using StepAIC (Step Akaike Information Criteria). Thirty-four RNAs were found to provide a plateau of predictive power ($t = 8 \times 10^{-18}$) for L1PA expression in ovarian cancer (Supplementary Table S2F). RNA features associated with elevated L1PA RNA levels included decreases in regulators of autophagy and lysosomal degradation (LAMTOR1, ATP6V0E1 and RAB1B) consistent with previous observations that autophagy degrades retrotransposon RNA (20). Notably, 32% of these RNAs are involved in oxidative phosphorylation, mitochondrial fission and mitochondrial translation. GO-terms associated with mitochondria and oxidative stress were the only ones statistically enriched in LINE-1 RNA predictive features for ovarian cancer.

We selected candidate genes and complexes from the lists above, including multiple RNA binding proteins (BAT1/DDX39B, TNRC6A, PNN, RNPC3, SETX and SNRNP70) and chromatin or DNA-modifying proteins (POU5F2 and CHD2) that could control expression of broad classes of retrotransposons. PNN, DDX39B, RNPC3 and SNRNP70 knockdown decreased *Alu* retrotransposition, while CHD2 augmented *Alu* retrotransposition (Figure 3D). It is possible these effects could be due to candidate genes affecting the transfected plasmid, or the splicing events required by this retrotransposition assay, but not by endogenous retrotransposons. In these cases, the candidate genes would not affect endogenous retrotransposons. To test the effect of candidates on retrotransposition-competent LINE-1 and *Alu* family members, RT-qPCR primers were designed to differentiate L1HS from other L1PA elements, and *AluYa5* and *AluYb8* from other *Alu* (Supplementary Figure S4). While knockdown of several of candidates had no significant impact on expression of retrotransposon RNA levels (RNPC3, SETX, DDX39B, TNRC6A, DGCR8, Supplementary Figure S5A and B), others including PNN, SNRNP70 and CHD2 did significantly decrease expression of LINE-1 and *Alu* RNAs (Figure 3E and F) suggesting they impact endogenous retrotransposons directly. The correlation of some RNAs with retrotransposon RNAs could be due altered expression of RNAs with embedded *Alu* or LINE-1 elements, and not independent retrotransposons. Despite this caveat, cumulatively our data suggests that analyzing mRNAs correlated with retrotransposon RNAs provides a bioinformatic screening strategy to identify candidate proteins impacting retrotransposons in tumors.

Retrotransposon control by genes frequently inactivated in ovarian cancer

We evaluated whether expression levels of any genes commonly lost or mutated in ovarian cancer also correlated with retrotransposon RNA levels, as these could control expression of retrotransposons in a broad subset of patients. Among genes frequently mutated in ovarian cancer (e.g. NF1, PAX8 and MECOM) (49), Breast cancer type 1 susceptibility protein (BRCA1) RNA levels emerged as having one of the strongest correlations with *Alu,* L1PA and L1PB levels ($r = 0.15$–0.19, Supplementary Table S2E). This correlation was less apparent in breast cancer (Supplementary Table S2G).

BRCA1 has reduced expression or activity due to deletion, mutation or hypermethylation of the gene in up to 23% of ovarian cancer tumors (49). As expected, ovarian tumors that exhibited loss of one or more copies of *BRCA1*, or hypermethylation of the *BRCA1* locus had reduced levels of *BRCA1* mRNA (Figure 4A and B). Levels of *BRCA1* mRNA in ovarian tumors significantly correlated with levels of LINE-1 and *AluY* RNA (Figure 4C and D). This suggested that BRCA1 may control levels of retrotransposon RNA in ovarian tumors.

BRCA1 increases levels of retrotransposon RNA, proteins and genomic insertions

BRCA1 promotes repair of double-strand DNA breaks via the homologous recombination pathway (HR) and occasionally through the non-homologous end-joining pathway (NHEJ) (50,51). BRCA1 also regulates transcription by binding directly to specific DNA sequences[46] and regulating RNA polymerases I, II and III (52–54).

RNA encoded by retrotransposition-competent LINE-1 elements (L1HS) and *AluY* elements was measured by RT-qPCR in *in vitro* cultures of spheroids generated from patient cancer cells with or without confirmed *BRCA1* mutations or deletions as previously described (19,55). Spheroid cultures from patients with loss of BRCA1 function had less LINE-1 and *AluY* RNA than cells with wild-type *BRCA1* genes (Figure 4E). This supports the hypothesis that loss of BRCA1 decreases retrotransposon RNA levels. To dissect the underlying mechanism, we utilized cellular models. Untransformed mouse ovarian surface epithelial cells with a single copy of *BRCA1* genetically deleted using a Cre-lox system (17), had 50% less *BRCA1* mRNA as expected (Figure 4F). Mouse cells do not harbor *Alu* elements, but LINE-1 RNA levels were significantly reduced in cells lacking a single copy of *BRCA1*, mimicking loss of BRCA1 in patients (Figure 4F). Similarly, LINE-1, *AluYa5* and *AluYb8* RNA levels were significantly reduced when BRCA1 was transiently knocked down in ES2 or HeLa cells using either of two independent BRCA1 siRNA sequences (Figure 4G and Supplementary Figure S6A). In addition, in either mouse ovarian epithelial cells or ES2 cells, loss of BRCA1 reduced levels of ORF1p and ORF2p proteins (Figure 4H and I). Northern blot with a single probe targeting the L1HS 5′UTR, or with multiple probes specific for L1HS demonstrated decreased levels of full-length (6000 kb) LINE-1 RNA when BRCA1 was depleted (Figure 4J). The data above demonstrates that levels of full length L1HS RNAs (Figure 4J) including the 5′UTR, ORF1 and ORF2 as well as the encoded proteins (Figure 4F–I) are decreased when BRCA1 expression is decreased. This demonstrates that BRCA1 controls levels of retrotransposon RNA and

proteins that are highly likely to be capable of retrotransposition.

To test whether BRCA1 also impacts retrotransposon insertions, LINE-1 and Alu retrotransposition reporter assays with exogenous promoters were employed (56,57). A version of the LINE-1 retrotransposition GFP reporter with two point mutations, which ablates retrotransposition was used as a negative control. When BRCA1 was transiently knocked down in ES2 and HEK 293T cells, significantly fewer retrotransposition events occurred (Figure 4K; Supplementary Figure S6B and C). For *Alu* retrotransposition assays a neomycin resistant reporter was used to avoid reporter-dependent artifacts. Similarly, when BRCA1 was transiently knocked down significantly fewer *Alu* retrotransposition events were observed (Figure 4L). This suggests that BRCA1 reduces LINE-1 and *Alu* retrotransposon RNA levels and retrotransposition via a mechanism that remains to be explored.

BRCA1 regulates retrotransposons independent of DNA damage repair

BRCA1 is involved in DNA double-strand breaks (DSB) repair mechanisms (58,59). LINE-1 reporters can induce DSB when transiently transfected and their retrotransposition is presumed to involve DNA repair mechanisms (60). Data on which DNA repair pathway is required for LINE-1 retrotransposition is conflicting (60–63), potentially due to myriad disruptions in DNA damage repair pathways that differ between cancer cell lines.

If BRCA1 was to impede genomic insertion of retrotransposons it would not be expected to have an impact on or decrease the amount of retrotransposon RNA. Transient silencing of key proteins in either HR or NHEJ pathways by 70–95% with siRNA (Rad50, Rad51, XRCC2, DMC1, MRE11 and XRCC6; Supplementary Figure S6D and E) did not phenocopy effects of BRCA1 silencing and reduce levels of LINE-1 RNA (Figure 5A and B). This suggests that BRCA1 regulates retrotransposon RNA levels by a mechanism other than DNA repair.

BRCA1 does not bind ORF1p or retrotransposon RNA to stabilize retrotransposon RNAs

Levels of LINE-1 and *Alu* RNAs and ORF1p were decreased when BRCA1 was depleted (Figure 4). ORF1p binds LINE-1 and *Alu* RNAs and may stabilize their RNAs. HA-ORF1p was not detected in immunoprecipitates of BRCA1, and BRCA1 was not detected in immunoprecipitates of HA-ORF1p (Supplementary Figure S6F). Therefore, BRCA1 does not bind ORF1p to regulate levels of retrotransposon RNAs.

Studies have shown BRCA1 can bind RNA (64) potentially including LINE-1 RNA (65). To test in our system if BRCA1 could bind and stabilize retrotransposon RNA, BRCA1 was immunoprecipitated in conditions to retain bound RNA. RNA was pulled down with a known RNA-binding protein (HuR) (66) (Supplementary Figure S6G), but no retrotransposon RNA was enriched in BRCA1 immunoprecipitates compared to immunoprecipitates of IgG controls (Figure 5C and Supplementary Figure S6H). This suggests BRCA1 does not bind retrotransposon RNA directly.

BRCA1 binds genomic LINE-1 copies and promotes transcription of retrotransposons

BRCA1 has been observed to bind DNA and promote the transcription of RNA by RNA polymerase I, II and III (52–54). We sought to assess whether BRCA1 increases levels of retrotransposon RNA by promoting their transcription. To define whether BRCA1 binds to DNA encoding and surrounding LINE-1 we first analyzed public ChIP data (B cells, Embryonic Stem Cell Line H1 and HepG2). Peaks of BRCA1 binding were mapped across the 146 intact and active LINE-1 elements found in L1Base (67). Peaks of BRCA1 binding within or in proximity to several active LINE-1 elements were observed (Supplementary Dataset 3). To experimentally confirm this, we performed BRCA1 ChIP. Chromatin fragments were confirmed to be largely under 250 bp (Figure 5D). A transcriptional pause site in β-Actin mRNA that is known to be bound by BRCA1 was detected in BRCA1 ChIP, whereas an intronic region of β-Actin mRNA not regulated by BRCA1 was not (68) (Figure 5D). DNA from the 5′ and 3′ ends of LINE-1 DNA as well as the central region of LINE-1 were enriched in BRCA1 ChIP compared to ChIP with control IgG in both ES2 and HeLa cell lines (Figure 5E and F). This suggests that BRCA1 binds to the genomic regions of LINE-1 (Figure 5D and F).

We hypothesized that BRCA1 binds genomic copies of LINE-1 to promote their transcription. To demonstrate whether BRCA1 affects transcription of retrotransposon RNA cells we provided a pulse of ethynyl-uridine to label nascent RNA, chased for 1 h and labeled RNA was captured on streptavidin-coated beads. *GAPDH* mRNA which across experimental systems has a half-life exceeding 12 h (69) was used for normalization. β-actin mRNA whose transcription is known to be promoted by BRCA1 (68) accumulated less in the chase period in cells depleted of BRCA1 (Figure 6A) validating the pulse-chase assay and the effect of BRCA1. Accumulation of nascent LINE-1 and *Alu* RNA were both significantly impeded by knockdown of BRCA1 (Figure 6B). This indicates that BRCA1 binds genomic regions of retrotransposons and increases transcription of LINE-1 and *Alu* RNA to promote retrotransposition (Figures 5D–F and 6A and B).

Evidence suggests that BRCA1 activates transcription after its activation by associating with elongating RNA polymerase II and regulating pausing of RNA polymerase II (70). In agreement, evidence here suggests that BRCA1 can promote LINE-1 activity independent of their endogenous promoters (Figure 4K and L) and associates with the body of LINE-1 sequences (Figure 5D–F). One mechanism by which BRCA1 promotes transcription is by promoting resolution of DNA–RNA hybrids called R-loops (68). DNA–RNA hybrids form during reverse transcription of LINE-1. R-loops are also often formed near promoters and slow transcription and BRCA1 can promote transcription of genes containing R loops (68). By resolving R-loops formed during transcription of retrotransposons BRCA1 could promote transcription of LINE-1 and *Alu*

RNA. If this was the case, the number of R-loops, containing retrotransposon DNA–RNA hybrids formed during transcription or reverse-transcription would increase when BRCA1 was depleted. DNA was fragmented with a cocktail of restriction enzymes and R-loops were pulled-down with the S9.6 monoclonal antibody. R-loops were enriched at known sites in RPL13A and eliminated by RNase H, which specifically degrades RNA–DNA hybrids (68) (Supplementary Figure S6I). A site known to contain few R-loops in EGR1 was poorly enriched in R-loops (Supplementary Figure S6I). R-loops at RPL13A accumulated when BRCA1 was depleted confirming the role of BRCA1 in resolving R-loops (Figure 6C). RNA–DNA hybrids containing LINE-1 sequences were also detected and eliminated by RNase H (Figure 6D). While BRCA1 siRNA knockdown increased R-loops at RPL13A, RNA–DNA hybrids at LINE-1 were significantly decreased (Figure 6C and D). This suggests BRCA1 does not resolve R-loops generated during LINE-1 transcription or reverse-transcription. Instead, the data shows that BRCA1 knockdown decreases LINE-1 RNA transcription (Figure 6D) and RNA levels (Figure 4), and this decreased transcription would lead to the formation of fewer DNA–RNA hybrids, or R-loops during LINE-1 transcription or reverse transcription.

The presented data harnessed the heterogeneity of tumors analyzed in The Cancer Genome Atlas to identify factors and pathways regulating retrotransposon RNA in the context of patient tumors. This provided new RNA-binding proteins (PNN, SNRNP70), transcription (BRCA1) and heterochromatin factors (CHD2), and pathways (viral response activation) controlling retrotransposon levels in ovarian and breast cancer. This underscores the complex control and effects of retrotransposons and suggests new mechanisms contributing to survival of ovarian cancer patients.

DISCUSSION

The regulation and impact of retrotransposons in various cancers is beginning to be uncovered. Sporadic reports have found that retrotransposons frequently disrupt tumor suppressors like *MYC* (71) or *ST18* (12), potentially due to the selection of these cells during tumor evolution. This does not appear to be a feature of the ovarian cancer samples analyzed here. Clusters of retrotransposon insertions were found surrounding HLA genes that could impact the immunogenicity of the tumor, and in EPHA3, which is frequently altered in cancer and has tumor suppressor properties (72). In general, disruption of tumor suppressors by retrotransposons was an infrequent, seemingly random, occurrence in ovarian cancer but in rare cases may have tumorigenic or tumor-promoting effects that impact patient survival.

Retrotransposons are also frequent at sites of genomic rearrangements, and the frequency of these may be increased by LINE-1 ORF2 protein, and transcription at these sites. For example, rearrangements in BRCA1 at an *Alu* element in intron 15 are linked to evolution in tumors of resistance to PARP inhibitors. Our data suggests that BRCA1 activity would promote transcription and ORF2 activity of retrotransposons, thereby increasing genomic rearrangements driven by retrotransposons.

Due to the lack of systematic effect of retrotransposon insertions, we aimed to understand the impact of retrotransposon expression levels in ovarian and breast cancer. Normally, TREX1 and RNase H eliminate retrotransposon intermediates like RNA–DNA hybrids to act as a homeostatic buffer preventing activation of STING-cGAS and production of type I Interferons. Mutations of TREX1 or RNase H cause accumulation of retrotransposon intermediates and an inflammatory response that manifests as Aicardi-Goutieres disease (73). Similarly, accumulation of retrotransposon intermediates caused by drugs inhibiting heterochromatin, or in senescent cells is associated with production of type I interferons and other inflammatory mediators (74,75). While levels of retrotransposon RNA were similar in ovarian and breast cancer (Figure 3A and B), type I Interferons were induced only in breast cancer alongside retrotransposon RNA and an inflammatory senescence-associated secretory phenotype was not apparent in either cancer (Figure 2E and H), despite the levels of retrotransposon RNAs being similar in both cancers (Figure 3A and B). This suggests that ovarian and breast tumors differ substantially in their capacity to eliminate or respond to retrotransposon intermediates. A previous report also noted heterogenous immune responses associated with retrotransposon expression among esophageal and gastrointestinal cancers (38). Our data suggests that type I Interferon activation by retrotransposons is insufficient to affect tumor growth or patient survival in breast cancer and does not measurably occur in ovarian cancer. This suggests that the complex network of gene expression correlated with LINE-1 RNA identified here predict survival of ovarian cancer patients in new ways independent of type I interferons.

Recent evidence demonstrated that in cell lines BRCA1 can suppress LINE-1 retrotransposition by influencing DNA repair events involved in their insertion into the genome (65,76). In contrast, we found that BRCA1 promotes transcription of endogenous LINE-1 RNA and increases the number of retrotransposition events. There are several differences between these studies that may account for their contrasting results. The studies which identified BRCA1 as a suppressor of LINE-1 insertions used Doxycycline-inducible LINE-1 overexpression plasmids and therefore were not positioned to identify effects on transcription of retrotransposons. In addition, doxycycline has extensive effects on cellular metabolism and transcription by affecting mitochondrial translation (77,78). In contrast, we focused on control of retrotransposon RNA levels produced from endogenous copies in patient tumors, patient tumor-derived spheroids, primary ovarian epithelial cells and multiple cell lines. Another difference between these studies is the methods used to study *BRCA1*. In the other studies, CRISPR was used to eliminate production of BRCA1, while we used more subtle tools including siRNA-mediated knockdown, single copy deletion of *BRCA1*, endogenous variation in *BRCA1* expression and mutated *BRCA1* in patient spheroids. It is possible that the effects of BRCA1 on DNA repair mechanisms involved in retrotransposon insertions in the genome only become apparent with complete elimination of *BRCA1* function. The

current evidence suggests that mutation of BRCA1 or loss of one copy of *BRCA1* impairs the transcription of new LINE-1 and *Alu* RNA independent of its roles in DNA repair or resolution of R-loops.

Loss of BRCA1 is tumorigenic. Normal levels of BRCA1 may maintain untransformed cells near a threshold of retrotransposon accumulation that could induce type I interferon responses and apoptosis. In cells which have lost BRCA1 activity, increased DNA damage may also cause decreases in retrotransposon RNA that also reduce type I interferons and apoptosis. These effects mediated in part via retrotransposon RNA may promote the emergence of tumorigenic cells in patients with BRCA1 loss of function.

The foundational mechanisms mediating LINE-1 transcription, replication and re-insertion into the genome have emerged over the preceding decades. These discoveries have largely been made using cell culture models that are easy to manipulate. Currently, a major challenge is to understand the physiological contexts where production of retrotransposon RNA and proteins, or genomic insertions of retrotransposons have impact on development and disease. This is particularly daunting due to the challenge of silencing or eliminating hundreds of copies of diverse retrotransposons or expressing them at physiologically relevant levels *in vivo* in higher mammals that share divergent retrotransposon families with humans. Patients and tumors have extensive genetic and environmental heterogeneity that can be exploited to identify the impacts of retrotransposons and common factors that regulate retrotransposons. As the current study demonstrates, analyzing RNAs that correlate closely with levels of retrotransposon RNA allows identification of factors and processes regulated by and regulating retrotransposons. A similar approach using Bayesian correlations could be applied to other processes of development and disease to identify the regulation and consequences of retrotransposon activation in physiological conditions in humans, such as in other cancers, Amyotrophic Lateral Sclerosis or Aicardi-Goutiere's syndrome.

DATA AVAILABILITY

All data are available from authors upon reasonable request.

SUPPLEMENTARY DATA

Supplementary Data are available at NAR Cancer Online.

ACKNOWLEDGEMENTS

The authors thank James Taylor for preparing probes for northern blots. The results published here are in whole or part based upon data generated by The Cancer Genome Atlas managed by the NCI and NHGRI. Information about TCGA can be found at http://cancergenome.nih.gov.

FUNDING

Qatar National Research Fund [QRLP9-G-3330014 to M.A.]; US Department of Defense CDMRP Ovarian Cancer Research Program [W81XWH-17-1-0212 to D.P.]; Canadian Cancer Society Research Institute [702978 to D.G.]; Canadian Institutes of Health Research [142174 to D.G.]; Canadian Institutes of Health Research [326557 to B.V.].
Conflict of interest statement. None declared.

REFERENCES

1. Kazazian,H.H. Jr and Moran,J. V (2017) Mobile DNA in health and disease. *N. Engl. J. Med.*, **377**, 361–370.
2. Cost,G.J., Feng,Q., Jacquier,A. and Boeke,J.D. (2002) Human L1 element target-primed reverse transcription in vitro. *EMBO J.*, **21**, 5899–5910.
3. Sanchez-Luque,F.J., Kempen,M.H.C., Gerdes,P., Vargas-Landin,D.B., Richardson,S.R., Troskie,R.L., Jesuadian,J.S., Cheetham,S.W., Carreira,P.E., Salvador-Palomeque,C. *et al.* (2019) LINE-1 evasion of epigenetic repression in humans. *Mol. Cell*, **75**, 590–604.
4. Athanikar,J.N., Badge,R.M. and Moran,J. V (2004) A YY1-binding site is required for accurate human LINE-1 transcription initiation. *Nucleic Acids Res.*, **32**, 3846–3855.
5. Yang,N., Zhang,L., Zhang,Y. and Kazazian,H.H. Jr (2003) An important role for RUNX3 in human L1 transcription and retrotransposition. *Nucleic Acids Res.*, **31**, 4929–4940.
6. Deininger,P. (2011) Alu elements: know the SINEs. *Genome Biol.*, **12**, 236–248.
7. Sudmant,P.H., Rausch,T., Gardner,E.J., Handsaker,R.E., Abyzov,A., Huddleston,J., Zhang,Y., Ye,K., Jun,G., Fritz,M.H.Y. *et al.* (2015) An integrated map of structural variation in 2,504 human genomes. *Nature*, **526**, 75–81.
8. Flasch,D.A., Macia,Á., Sánchez,L., Ljungman,M., Heras,S.R., García-Pérez,J.L., Wilson,T.E. and Moran,J. V. (2019) Genome-wide de novo L1 retrotransposition connects endonuclease activity with replication. *Cell*, **177**, 837–851.
9. Sultana,T., van Essen,D., Siol,O., Bailly-Bechet,M., Philippe,C., Zine El Aabidine,A., Pioger,L., Nigumann,P., Saccani,S., Andrau,J.C. *et al.* (2019) The landscape of L1 retrotransposons in the human genome is shaped by Pre-insertion sequence biases and post-insertion selection. *Mol. Cell*, **74**, 555–570.
10. Goodier,J.L. (2016) Restricting retrotransposons: a review. *Mob. DNA*, **7**, 16–46.
11. Miki,Y., Nishisho,I., Horii,A., Miyoshi,Y., Utsunomiya,J., Kinzler,K.W., Vogelstein,B. and Nakamura,Y. (1992) Disruption of the APC gene by a retrotransposal insertion of L1 sequence in a colon cancer. *Cancer Res.*, **52**, 643–645.
12. Shukla,R., Upton,K.R., Munoz-Lopez,M., Gerhardt,D.J., Fisher,M.E., Nguyen,T., Brennan,P.M., Baillie,J.K., Collino,A., Ghisletti,S. *et al.* (2013) Endogenous retrotransposition activates oncogenic pathways in hepatocellular carcinoma. *Cell*, **153**, 101–111.
13. Tang,Z., Steranka,J.P., Ma,S., Grivainis,M., Rodic,N., Huang,C.R., Shih,I.M., Wang,T.L., Boeke,J.D., Fenyo,D. *et al.* (2017) Human transposon insertion profiling: Analysis, visualization and identification of somatic LINE-1 insertions in ovarian cancer. *Proc. Natl. Acad. Sci. U.S.A.*, **114**, E733–E740.
14. Thomas,C.A., Tejwani,L., Trujillo,C.A., Negraes,P.D., Herai,R.H., Mesci,P., Macia,A., Crow,Y.J. and Muotri,A.R. (2017) Modeling of TREX1-Dependent autoimmune disease using human stem cells highlights L1 accumulation as a source of neuroinflammation. *Cell Stem Cell*, **21**, 319–331.
15. De Cecco,M., Ito,T., Petrashen,A.P., Elias,A.E., Skvir,N.J., Criscione,S.W., Caligiana,A., Brocculi,G., Adney,E.M., Boeke,J.D. *et al.* (2019) L1 drives IFN in senescent cells and promotes age-associated inflammation. *Nature*, **566**, 73–78.
16. Guler,G.D., Tindell,C.A., Pitti,R., Wilson,C., Nichols,K., KaiWai Cheung,T., Kim,H.J., Wongchenko,M., Yan,Y., Haley,B. *et al.* (2017) Repression of stress-induced LINE-1 expression protects cancer cell subpopulations from lethal drug exposure. *Cancer Cell*, **32**, 221–237.
17. Gamwell,L.F., Collins,O. and Vanderhyden,B.C. (2012) The mouse ovarian surface epithelium contains a population of LY6A (SCA-1) expressing progenitor cells that are regulated by ovulation-associated factors. *Biol. Reprod.*, **87**, 80–90.

18. Kroutter,E.N., Belancio,V.P., Wagstaff,B.J. and Roy-Engel,A.M. (2009) The RNA polymerase dictates ORF1 requirement and timing of LINE and SINE retrotransposition. *PLos Genet.*, **5**, e1000458.
19. Pepin,D., Sosulski,A., Zhang,L., Wang,D., Vathipadiekal,V., Hendren,K., Coletti,C.M., Yu,A., Castro,C.M., Birrer,M.J. *et al.* (2015) AAV9 delivering a modified human Mullerian inhibiting substance as a gene therapy in patient-derived xenografts of ovarian cancer. *Proc. Natl. Acad. Sci. U.S.A.*, **112**, E4418–E4427.
20. Guo,H., Chitiprolu,M., Gagnon,D., Meng,L., Perez-Iratxeta,C., Lagace,D. and Gibbings,D. (2014) Autophagy supports genomic stability by degrading retrotransposon RNA. *Nat. Commun.*, **5**, 5276–5287.
21. Deininger,P. and Belancio,V.P. (2016) Detection of LINE-1 RNAs by northern blot. In: *Methods in Molecular Biology*. Humana Press, NY, Vol. **1400**, pp. 223–236.
22. Rio,D.C. (2015) Northern blots: capillary transfer of RNA from Agarose gels and filter hybridization using standard stringency conditions. *Cold Spring Harb. Protoc.*, **2015**, 306–313.
23. Llave,C., Xie,Z., Kasschau,K.D. and Carrington,J.C. (2002) Cleavage of Scarecrow-like mRNA targets directed by a class of Arabidopsis miRNA. *Science (80-.).*, **297**, 2053–2056.
24. Sambrook,J. and Green,M.R. (2012) In: *Molecular Cloning: A Laboratory Manual*. 4th edn, Cold Spring Harbor Laboratory press, NY.
25. Wiehle,L. and Breiling,A. (2016) Chromatin Immunoprecipitation. *Methods Mol. Biol.*, **1480**, 7–21.
26. Sanz,L.A. and Chedin,F. (2019) High-resolution, strand-specific R-loop mapping via S9.6-based DNA-RNA immunoprecipitation and high-throughput sequencing. *Nat. Protoc.*, **14**, 1734–1755.
27. Gardner,E.J., Lam,V.K., Harris,D.N., Chuang,N.T., Scott,E.C., Pittard,W.S., Mills,R.E. and Genomes Project, C.Genomes Project, C. and Devine,S.E. (2017) The Mobile Element Locator Tool (MELT): population-scale mobile element discovery and biology. *Genome Res.*, **27**, 1916–1929.
28. Mir,A.A., Philippe,C. and Cristofari,G. (2015) euL1db: the European database of L1HS retrotransposon insertions in humans. *Nucleic Acids Res.*, **43**, D43–D47.
29. Genomes Project, C., Auton,A., Brooks,L.D., Durbin,R.M., Garrison,E.P., Kang,H.M., Korbel,J.O., Marchini,J.L., McCarthy,S., McVean,G.A. *et al.* (2015) A global reference for human genetic variation. *Nature*, **526**, 68–74.
30. Kuusisto,K.M., Akinrinade,O., Vihinen,M., Kankuri-Tammilehto,M., Laasanen,S.L. and Schleutker,J. (2013) copy number variation analysis in familial BRCA1/2-negative Finnish breast and ovarian cancer. *PLoS One*, **8**, e71802.
31. Schuster,H., Peper,J.K., Bosmuller,H.C., Rohle,K., Backert,L., Bilich,T., Ney,B., Loffler,M.W., Kowalewski,D.J., Trautwein,N. *et al.* (2017) The immunopeptidomic landscape of ovarian carcinomas. *Proc. Natl. Acad. Sci. U.S.A.*, **114**, E9942–E9951.
32. Hart,T., Chandrashekhar,M., Aregger,M., Steinhart,Z., Brown,K.R., MacLeod,G., Mis,M., Zimmermann,M., Fradet-Turcotte,A., Sun,S. *et al.* (2015) High-resolution CRISPR screens reveal fitness genes and genotype-specific cancer liabilities. *Cell*, **163**, 1515–1526.
33. Lever,J., Zhao,E.Y., Grewal,J., Jones,M.R. and Jones,S.J.M. (2019) CancerMine: a literature-mined resource for drivers, oncogenes and tumor suppressors in cancer. *Nat. Methods*, **16**, 505–507.
34. Jurka,J., Kapitonov,V.V, Pavlicek,A., Klonowski,P., Kohany,O. and Walichiewicz,J. (2005) Repbase Update, a database of eukaryotic repetitive elements. *Cytogenet. Genome Res.*, **110**, 462–467.
35. Bao,W., Kojima,K.K. and Kohany,O. (2015) Repbase Update, a database of repetitive elements in eukaryotic genomes. *Mob. DNA*, **6**, 11–17.
36. Criscione,S.W., Zhang,Y., Thompson,W., Sedivy,J.M. and Neretti,N. (2014) Transcriptional landscape of repetitive elements in normal and cancer human cells. *BMC Genomics*, **15**, 583–600.
37. Roulois,D., Loo Yau,H., Singhania,R., Wang,Y., Danesh,A., Shen,S.Y., Han,H., Liang,G., Jones,P.A., Pugh,T.J. *et al.* (2015) DNA-Demethylating agents target colorectal cancer cells by inducing viral mimicry by endogenous transcripts. *Cell*, **162**, 961–973.
38. Jung,H., Choi,J.K. and Lee,E.A. (2018) Immune signatures correlate with L1 retrotransposition in gastrointestinal cancers. *Genome Res.*, **28**, 1136–1146.
39. Wang,X., Park,J., Susztak,K., Zhang,N.R. and Li,M. (2019) Bulk tissue cell type deconvolution with multi-subject single-cell expression reference. *Nat. Commun.*, **10**, 380–389.
40. Fort,M.M., Cheung,J., Yen,D., Li,J., Zurawski,S.M., Lo,S., Menon,S., Clifford,T., Hunte,B., Lesley,R. *et al.* (2001) IL-25 induces IL-4, IL-5, and IL-13 and Th2-associated pathologies in vivo. *Immunity*, **15**, 985–995.
41. Sun,X., Wang,X., Tang,Z., Grivainis,M., Kahler,D., Yun,C., Mita,P., Fenyö,D. and Boeke,J.D. (2018) Transcription factor profiling reveals molecular choreography and key regulators of human retrotransposon expression. *Proc. Natl. Acad. Sci. U.S.A.*, **115**, E5526–E5535.
42. Kumar,P.P., Mehta,S., Purbey,P.K., Notani,D., Jayani,R.S., Purohit,H.J., Raje,D. V, Ravi,D.S., Bhonde,R.R., Mitra,D. *et al.* (2007) SATB1-binding sequences and Alu-like motifs define a unique chromatin context in the vicinity of human immunodeficiency virus type 1 integration sites. *J. Virol.*, **81**, 5617–5627.
43. Ashburner,M., Ball,C.A., Blake,J.A., Botstein,D., Butler,H., Cherry,J.M., Davis,A.P., Dolinski,K., Dwight,S.S., Eppig,J.T. *et al.* (2000) Gene ontology: tool for the unification of biology. The Gene Ontology Consortium. *Nat. Genet.*, **25**, 25–29.
44. The Gene Ontology, C. (2019) The Gene Ontology Resource: 20 years and still GOing strong. *Nucleic Acids Res.*, **47**, D330–D338.
45. Raudvere,U., Kolberg,L., Kuzmin,I., Arak,T., Adler,P., Peterson,H. and Vilo,J. (2019) g:Profiler: a web server for functional enrichment analysis and conversions of gene lists (2019 update). *Nucleic Acids Res.*, **47**, W191–W198.
46. Krug,L., Chatterjee,N., Borges-Monroy,R., Hearn,S., Liao,W.W., Morrill,K., Prazak,L., Rozhkov,N., Theodorou,D., Hammell,M. *et al.* (2017) Retrotransposon activation contributes to neurodegeneration in a Drosophila TDP-43 model of ALS. *PLos Genet.*, **13**, e1006635.
47. Liu,E.Y., Russ,J., Cali,C.P., Phan,J.M., Amlie-Wolf,A. and Lee,E.B. (2019) Loss of Nuclear TDP-43 is associated with decondensation of LINE retrotransposons. *Cell Rep.*, **27**, 1409–1421.
48. Pereira,G.C., Sanchez,L., Schaughency,P.M., Rubio-Roldan,A., Choi,J.A., Planet,E., Batra,R., Turelli,P., Trono,D., Ostrow,L.W. *et al.* (2018) Properties of LINE-1 proteins and repeat element expression in the context of amyotrophic lateral sclerosis. *Mob. DNA*, **9**, 35–65.
49. Cancer Genome Atlas Research, N. (2011) Integrated genomic analyses of ovarian carcinoma. *Nature*, **474**, 609–615.
50. Escribano-Diaz,C., Orthwein,A., Fradet-Turcotte,A., Xing,M., Young,J.T., Tkac,J., Cook,M.A., Rosebrock,A.P., Munro,M., Canny,M.D. *et al.* (2013) A cell cycle-dependent regulatory circuit composed of 53BP1-RIF1 and BRCA1-CtIP controls DNA repair pathway choice. *Mol. Cell*, **49**, 872–883.
51. Bau,D.T., Fu,Y.P., Chen,S.T., Cheng,T.C., Yu,J.C., Wu,P.E. and Shen,C.Y. (2004) Breast cancer risk and the DNA double-strand break end-joining capacity of nonhomologous end-joining genes are affected by BRCA1. *Cancer Res.*, **64**, 5013–5019.
52. Anderson,S.F., Schlegel,B.P., Nakajima,T., Wolpin,E.S. and Parvin,J.D. (1998) BRCA1 protein is linked to the RNA polymerase II holoenzyme complex via RNA helicase A. *Nat. Genet.*, **19**, 254–256.
53. Veras,I., Rosen,E.M. and Schramm,L. (2009) Inhibition of RNA polymerase III transcription by BRCA1. *J. Mol. Biol.*, **387**, 523–531.
54. Johnston,R., D'Costa,Z., Ray,S., Gorski,J., Harkin,D.P., Mullan,P. and Panov,K.I. (2016) The identification of a novel role for BRCA1 in regulating RNA polymerase I transcription. *Oncotarget*, **7**, 68097–68110.
55. Sosulski,A., Horn,H., Zhang,L., Coletti,C., Vathipadiekal,V., Castro,C.M., Birrer,M.J., Nagano,O., Saya,H., Lage,K. *et al.* (2016) CD44 splice variant v8-10 as a marker of serous ovarian cancer prognosis. *PLoS One*, **11**, e0156595.
56. Moran,J. V, Holmes,S.E., Naas,T.P., DeBerardinis,R.J., Boeke,J.D. and Kazazian,H.H. Jr (1996) High frequency retrotransposition in cultured mammalian cells. *Cell*, **87**, 917–927.
57. Ostertag,E.M., Prak,E.T., DeBerardinis,R.J., Moran,J.V. and Kazazian,H.H. Jr (2000) Determination of L1 retrotransposition kinetics in cultured cells. *Nucleic Acids Res.*, **28**, 1418–1423.
58. Wang,Y., Cortez,D., Yazdi,P., Neff,N., Elledge,S.J. and Qin,J. (2000) BASC, a super complex of BRCA1-associated proteins involved in the recognition and repair of aberrant DNA structures. *Genes Dev.*, **14**, 927–939.

59. Bau,D.T., Mau,Y.C. and Shen,C.Y. (2006) The role of BRCA1 in non-homologous end-joining. *Cancer Lett.*, **240**, 1–8.
60. Babushok,D. V. and Kazazian,H.H. (2007) Progress in understanding the biology of the human mutagen LINE-1. *Hum. Mutat.*, **28**, 527–539.
61. Coufal,N.G., Garcia-Perez,J.L., Peng,G.E., Marchetto,M.C., Muotri,A.R., Mu,Y., Carson,C.T., Macia,A., Moran,J.V. and Gage,F.H. (2011) Ataxia telangiectasia mutated (ATM) modulates long interspersed element-1 (L1) retrotransposition in human neural stem cells. *Proc. Natl. Acad. Sci. U.S.A.*, **108**, 20382–20387.
62. Suzuki,J., Yamaguchi,K., Kajikawa,M., Ichiyanagi,K., Adachi,N., Koyama,H., Takeda,S. and Okada,N. (2009) Genetic evidence that the non-homologous end-joining repair pathway is involved in LINE retrotransposition. *PLos Genet.*, **5**, e1000461.
63. Gasior,S.L., Wakeman,T.P., Xu,B. and Deininger,P.L. (2006) The human LINE-1 retrotransposon creates DNA double-strand breaks. *J. Mol. Biol.*, **357**, 1383–1393.
64. Ganesan,S., Silver,D.P., Greenberg,R.A., Avni,D., Drapkin,R., Miron,A., Mok,S.C., Randrianarison,V., Brodie,S., Salstrom,J. *et al.* (2002) BRCA1 supports XIST RNA concentration on the inactive X chromosome. *Cell*, **111**, 393–405.
65. Mita,P., Sun,X., Fenyö,D., Kahler,D.J., Li,D., Agmon,N., Wudzinska,A., Keegan,S., Bader,J.S., Yun,C. *et al.* (2020) BRCA1 and S phase DNA repair pathways restrict LINE-1 retrotransposition in human cells. *Nat. Struct. Mol. Biol.*, **27**, 179–191.
66. Lopez de Silanes,I., Zhan,M., Lal,A., Yang,X. and Gorospe,M. (2004) Identification of a target RNA motif for RNA-binding protein HuR. *Proc. Natl. Acad. Sci. U.S.A.*, **101**, 2987–2992.
67. Penzkofer,T., Jäger,M., Figlerowicz,M., Badge,R., Mundlos,S., Robinson,P.N. and Zemojtel,T. (2017) L1Base 2: more retrotransposition-active LINE-1s, more mammalian genomes. *Nucleic Acids Res.*, **45**, D68–D73.
68. Hatchi,E., Skourti-Stathaki,K., Ventz,S., Pinello,L., Yen,A., Kamieniarz-Gdula,K., Dimitrov,S., Pathania,S., McKinney,K.M., Eaton,M.L. *et al.* (2015) BRCA1 recruitment to transcriptional pause sites is required for R-loop-driven DNA damage repair. *Mol. Cell*, **57**, 636–647.
69. Tani,H., Mizutani,R., Salam,K.A., Tano,K., Ijiri,K., Wakamatsu,A., Isogai,T., Suzuki,Y. and Akimitsu,N. (2012) Genome-wide determination of RNA stability reveals hundreds of short-lived noncoding transcripts in mammals. *Genome Res.*, **22**, 947–956.
70. Lane,T.F. (2004) BRCA1 and transcription. *Cancer Biol. Ther.*, **3**, 528–533.
71. Morse,B., Rotherg,P.G., South,V.J., Spandorfer,J.M. and Astrin,S.M. (1988) Insertional mutagenesis of the myc locus by a LINE-1 sequence in a human breast carcinoma. *Nature*, **333**, 87–90.
72. Peng,J., Wang,Q., Liu,H., Ye,M., Wu,X. and Guo,L. (2016) EPHA3 regulates the multidrug resistance of small cell lung cancer via the PI3K/BMX/STAT3 signaling pathway. *Tumour Biol.*, **37**, 11959–11971.
73. Benitez-Guijarro,M., Lopez-Ruiz,C., Tarnauskaite,Z., Murina,O., Mian Mohammad,M., Williams,T.C., Fluteau,A., Sanchez,L., Vilar-Astasio,R., Garcia-Canadas,M. *et al.* (2018) RNase H2, mutated in Aicardi-Goutieres syndrome, promotes LINE-1 retrotransposition. *EMBO J.*, **37**, e98506.
74. Saito,Y., Nakaoka,T., Sakai,K., Muramatsu,T., Toshimitsu,K., Kimura,M., Kanai,T., Sato,T. and Saito,H. (2016) Inhibition of DNA methylation suppresses intestinal tumor organoids by inducing an anti-viral response. *Sci. Rep.*, **6**, 25311–25320.
75. Rooney,M.S., Shukla,S.A., Wu,C.J., Getz,G. and Hacohen,N. (2015) Molecular and genetic properties of tumors associated with local immune cytolytic activity. *Cell*, **160**, 48–61.
76. Liu,N., Lee,C.H., Swigut,T., Grow,E., Gu,B., Bassik,M.C. and Wysocka,J. (2018) Selective silencing of euchromatic L1s revealed by genome-wide screens for L1 regulators. *Nature*, **553**, 228–232.
77. Moullan,N., Mouchiroud,L., Wang,X., Ryu,D., Williams,E.G., Mottis,A., Jovaisaite,V., Frochaux,M. V., Quiros,P.M., Deplancke,B. *et al.* (2015) Tetracyclines disturb mitochondrial function across eukaryotic models: a call for caution in biomedical research. *Cell Rep.*, **10**, 1681–1691.
78. Houtkooper,R.H., Mouchiroud,L., Ryu,D., Moullan,N., Katsyuba,E., Knott,G., Williams,R.W. and Auwerx,J. (2013) Mitonuclear protein imbalance as a conserved longevity mechanism. *Nature*, **497**, 451–457.